[CANCER RESEARCH 64, 2496–2501, April 1, 2004]

Molecular Classification and Survival Prediction in Human Gliomas Based on Proteome Analysis

Yasuo Iwadate,[1] Tsukasa Sakaida,[1] Takaki Hiwasa,[2] Yuichiro Nagai,[3] Hiroshi Ishikura,[3] Masaki Takiguchi,[2] Akira Yamaura[1]

Departments of [1]Neurological Surgery, [2]Biochemistry & Genetics, and [3]Molecular Pathology, Chiba University Graduate School of Medicine, Chiba, Japan

ABSTRACT

The biological features of gliomas, which are characterized by highly heterogeneous biological aggressiveness even in the same histological category, would be precisely described by global gene expression data at the protein level. We investigated whether proteome analysis based on two-dimensional gel electrophoresis and matrix-assisted laser desorption/ionization time-of-flight mass spectrometry can identify differences in protein expression between high- and low-grade glioma tissues. Proteome profiling patterns were compared in 85 tissue samples: 52 glioblastoma multiforme, 13 anaplastic astrocytomas, 10 atrocytomas, and 10 normal brain tissues. We could completely distinguish the normal brain tissues from glioma tissues by cluster analysis based on the proteome profiling patterns. Proteome-based clustering significantly correlated with the patient survival, and we could identify a biologically distinct subset of astrocytomas with aggressive nature. Discriminant analysis extracted a set of 37 proteins differentially expressed based on histological grading. Among them, many of the proteins that were increased in high-grade gliomas were categorized as signal transduction proteins, including small G-proteins. Immunohistochemical analysis confirmed the expression of identified proteins in glioma tissues. The present study shows that proteome analysis is useful to develop a novel system for the prediction of biological aggressiveness of gliomas. The proteins identified here could be novel biomarkers for survival prediction and rational targets for antiglioma therapy.

INTRODUCTION

The extensive heterogeneity of astrocytic tumors has made their pathological classification rather difficult; some identical low-grade astrocytomas progress to glioblastoma, whereas others persist in a dormant state for many years. Although several genetic aberrations and gene expression changes have been identified as associated with oncogenesis and malignant progression of the astrocytic tumors (1), their contribution to the clinical classification of gliomas has been limited. More comprehensive characterization of the gene expression that may correlate with the clinical behavior of gliomas is needed to establish an accurate molecular classification to predict the prognosis and treatment response of patients.

Molecular expression profiles using oligonucleotides or cDNA-based microarrays have been used to derive a useful molecular-based classification for the choice of treatment in several types of human cancers (2, 3). Gene expression profiles have identified many genes with distinct expression patterns among different histological types and grades of intracerebral gliomas (4–6). However, biological systems comprise protein components resulting from transcriptional and post-transcriptional control, post-translational modifications, and shifts in proteins among the different cellular compartments. These properties cannot be analyzed by microarray systems at the RNA level, whereas proteome analysis such as high-resolution two-dimensional gel electrophoresis (2DE) allows separation and visualization of the protein contents of a cellular sample (7). The recent introduction of commercially available immobilized ampholyte pH gradients, more standardized 2DE methods, and bioinformatics protein databases now make it more feasible to screen tumor-related global protein changes on a genome-wide scale (8, 9).

In this study, we examined several human glioma specimens, using 2DE and matrix-assisted laser desorption/ionization time-of-flight mass spectrometry to compare proteome profiling patterns between low- and high-grade tumors. The results showed that proteome-based clustering of gliomas significantly correlated with patient survival. We also identified a group of proteins that were differentially expressed in proportion to the degree of histological grading, which might be novel biomarkers to predict the clinical aggressiveness of gliomas and rational targets for antiglioma therapy.

MATERIALS AND METHODS

Tissue Specimens. After obtaining written informed consent from the patients or guardians, we analyzed 75 surgically resected human glioma tissues from newly diagnosed cases, along with 10 normal brain tissues. The normal brain tissues were obtained from patients undergoing resection of extra-axial brain tumors or epilepsy surgery. The resected tumors or normal brain samples were snap-frozen in liquid nitrogen and stored at −80°C for protein extraction immediately after surgical resection. The other portion of the tumor was fixed in 10% formaldehyde and embedded in paraffin for histopathological diagnosis. Of the 75 glioma tissues, 52 were classified as glioblastoma multiforme (GM; grade IV), 13 as anaplastic astrocytoma (grade III), and 10 samples as astrocytoma (grade II) by a neuropathologist according to the WHO criteria. The protocol of this experimental study was approved by the Institutional Review Board.

2DE. The frozen samples were mechanically homogenized in lysis buffer containing 30 mM Tris-HCl (pH 7.5), 150 mM NaCl, 1% Triton X-100, 10% glycerol, and protease inhibitor cocktail to generate protein lysates. Total protein concentrations were normalized to 1 μg/μl for all samples. Each protein sample (100 μg) was lyophilized and then mixed with sample buffer containing 7 M urea, 2 M thiourea, 4% (w/v) 3-[(3-cholamidopropyl)dimethylammonio]-1-propanesulfonic acid (CHAPS), and 1% (w/v) DTT. Isoelectric focusing for the first dimension of protein separation was performed with a Multiphore II electrophoresis system (Amersham Biosciences, Piscataway, NJ). Immobiline Dry IPG strips (7 cm, pH 3–10 nonlinear IPG strips; Amersham Biosciences) were rehydrated overnight with the sample/rehydration buffer mixture. The strips were subjected to electrophoresis using a ramping IPG strip (200–5000 V) focusing algorithm. After the isoelectric focusing, the gel strips were equilibrated with SDS equilibration buffer and electrophoresed in vertical SDS-PAGE slab gels containing 12.5% acrylamide. The gels were stained with the Silver Quest silver staining kit, which was compatible with mass spectrometry (Invitrogen Japan, K.K., Tokyo, Japan).

Image Analysis of 2DE Gels. Silver-stained gels were analyzed with the Phoretix 2D Advanced software (Version 5.01; Nonlinear Dynamic, Ltd., Newcastle, United Kingdom). Gel images from 10 samples of normal brain tissues were matched to generate a composite reference image including most of the possible spots. The total integrated spot volumes, the average volume of individual spots, and the SD were calculated, with the volume of the internal

Received 5/9/03; revised 11/4/03; accepted 1/20/04.

Grant support: Supported in part by a Grant-in-Aid for Scientific Research from the Japan Society for the Promotion of Science and a Grant-in-Aid for Scientific Research on priority areas from the Minister of Education, Culture, Sports, Science and Technology of Japan.

The costs of publication of this article were defrayed in part by the payment of page charges. This article must therefore be hereby marked *advertisement* in accordance with 18 U.S.C. Section 1734 solely to indicate this fact.

Requests for reprints: Yasuo Iwadate, Department of Neurological Surgery, Chiba University Graduate School of Medicine, 1-8-1, Inohana, Chuo-ku, Chiba 260-8670, Japan. Phone: 81-43-226-2158; Fax: 81-43-226-2159; E-mail: iwadate@med.m.chiba-u.ac.jp.

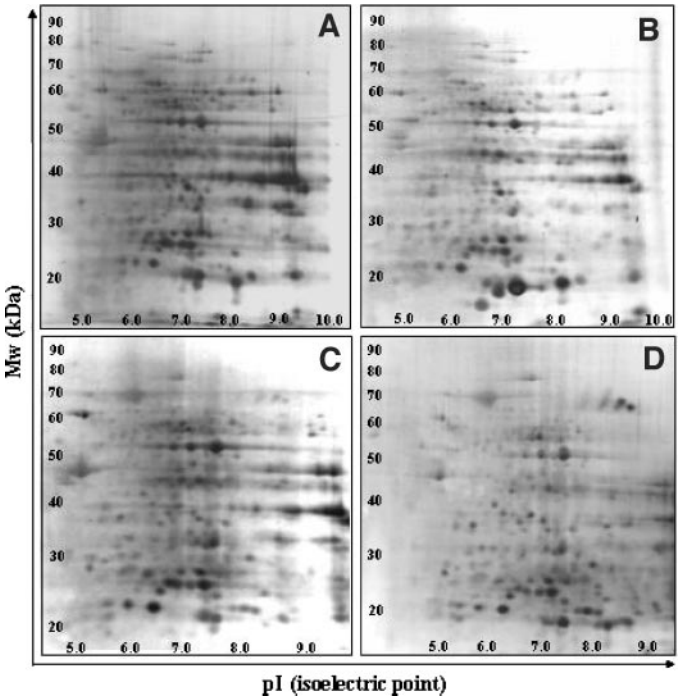

Fig. 1. Representative two-dimensional electrophoresis gels of each histological type. *A*, normal brain tissue; *B*, astrocytoma; *C*, anaplastic astrocytoma; *D*, glioblastoma multiforme. After isoelectric focusing for the first dimension of protein separation, the gel strips were electrophoresed in vertical SDS-PAGE slab gels and then stained with silver. Although the basic spot distribution patterns are similar among various histological grades, many protein spots were differentially expressed. *Mw*, molecular weight.

standard (keratin-1) used for normalization. To maximize the chance of detecting tumor-specific protein alterations, we also directly visually analyzed the gels. We compared the proteome profiles of the reference gel with the tumor gel; only spots that were present on the reference gel and completely absent from the matched gel (on-off changes) were defined as altered.

Matrix-Assisted Laser Desorption/Ionization Time-of-Flight Mass Spectrometry. The protein spots were excised from the gels, and in-gel digestion was performed with an enzyme solution containing 50 mM NH_4HCO_3, 5 mM $CaCl_2$, and 12.5 ng/μl trypsin. Aliquots of the purified samples were spotted on matrix crystals of α-cyano-4-hydroxyl-cinnamic acid on a stainless steel target and air dried. Mass determinations were performed on the AXIMA-CFR mass spectrometer (Shimadzu Co. Ltd., Kyoto, Japan). The proteins were identified by the peptide mass fingerprinting method, using Mascot Search on the Web (Matrix Science, Ltd., London, United Kingdom).

Immunohistochemical Analysis. Immunohistochemical analysis was performed on formalin-fixed, paraffin-embedded sections. The primary antibodies used were rabbit polyclonal anti-cAMP-responsive element binding protein-1 antibody (1:200 dilution), mouse monoclonal anti-Rho A antibody (1:100 dilution), rabbit polyclonal anti-Rac1 antibody (1:200 dilution), goat polyclonal anti-GRP78 antibody (1:100 dilution), and goat polyclonal antienolase antibody (1:100 dilution), all from Santa Cruz Biotechnology (Santa Cruz, CA). The sections were incubated with the antibodies overnight followed by incubation with biotinylated secondary antibodies (DakoCytomation, Copenhagen, Denmark). The bound antibodies were visualized with avidin–biotinylated peroxidase complex and diaminobenzidine tetrachloride.

Statistical Analysis. We carried out hierarchical cluster analysis for the tissue specimens based on the proteome profiling patterns in the 2DE gels. The squared Euclidean distance based on the standardized variables was used to calculate the distance between any two samples, and agglomerative hierarchical cluster analysis was performed using the method of complete linkage (SPSS, Inc., Chicago, IL). Kaplan–Meier survival curves were generated with StatView software (SAS Institute Inc., Cary, NC), and the survival periods were compared using the log-rank test. To screen out proteins that significantly affected histological grading, we used discriminant analysis (SPSS Inc.).

RESULTS

Proteome Profiling Patterns of Normal Brain Tissues and Gliomas. We comprehensively analyzed the protein expression patterns in 75 glioma specimens by use of a 2DE technology with immobilized pH gradients (Fig. 1). Approximately 350 protein spots were identified on each gel by a conservative spot selection software algorithm based on certain spot intensities. Many protein spots were differentially expressed among samples (Fig. 2). A composite reference gel of the 10 normal brain tissues contained a total of 631 protein spots. Gel comparisons between the reference gel and the gels from each glioma specimen revealed matching means of 64 $\pm$ 6.2% for astrocytoma and 47 $\pm$ 4.9% for GM ($P < 0.05$). Among the spots on the reference gel, 181 protein spots (28.7%) did not match with any spot on other gels from glioma tissues. These proteins may be specifically translated and functional in the normal brain. Among the 631 protein spots on the reference gel, 257 (40.7%) were found on more than two gels from glioma tissues, and many of the remaining unmatched protein spots appeared only on one gel, suggesting that the tumor-deregulated proteins were to a large extent sample specific and were proteolytic fragments or post-translationally modified proteins.

Cluster Analysis of Proteome Profiling Patterns of Human Gliomas. We performed hierarchical cluster analysis of the 75 tumor specimens and the 10 normal brain samples based on the presence or absence of the 257 protein spots to characterize the proteome profiling patterns associated with variable biological aggressiveness in the human gliomas. A dendrogram in the sample axis is shown in Fig. 3*A*. The samples taken from the normal brain tissues were completely categorized into single tissue-specific branches, indicating the validity and clinical significance of the proteome analysis. Seven astrocytoma samples were clustered in an area close to the normal brain tissues, and the patients manifested favorable clinical courses without recurrence. In contrast, two of the other three patients, with astrocytomas that clustered away from the normal brain tissues, had recurrences

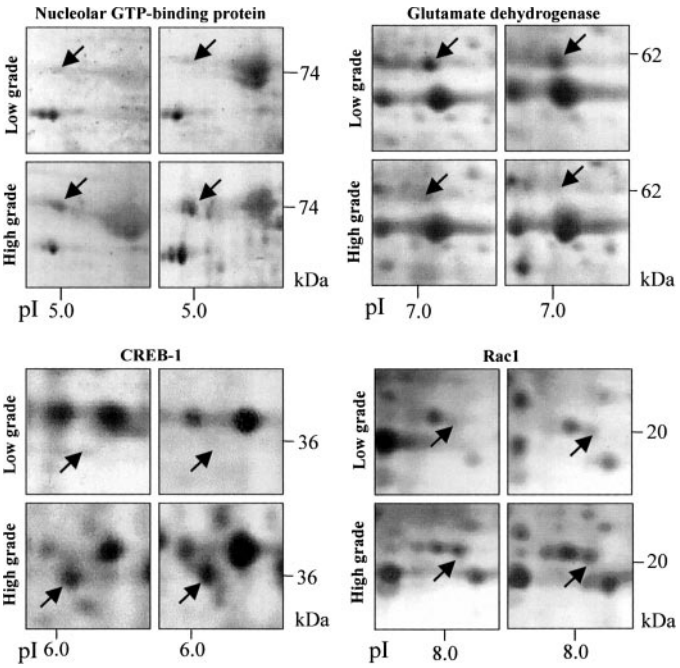

Fig. 2. Protein spots differentially expressed between low- and high-grade astrocytomas. Among 37 protein spots extracted by discriminant analysis with statistical significance, 4 representative protein spots are shown: nucleolar GTP-binding protein (*upper left*; 74.1 kDa; pI 5.04; $P = 0.0283$), glutamate dehydrogenase (*upper right*; 61.3 kDa; pI 7.26; $P = 0.0063$), cAMP-responsive element binding protein-1 (*CREB-1*; *lower left*; 36.6 kDa; pI 6.20; $P = 0.0032$), and Rac1 (*lower right*; 21.5 kDa; pI 8.10; $P = 0.0001$).

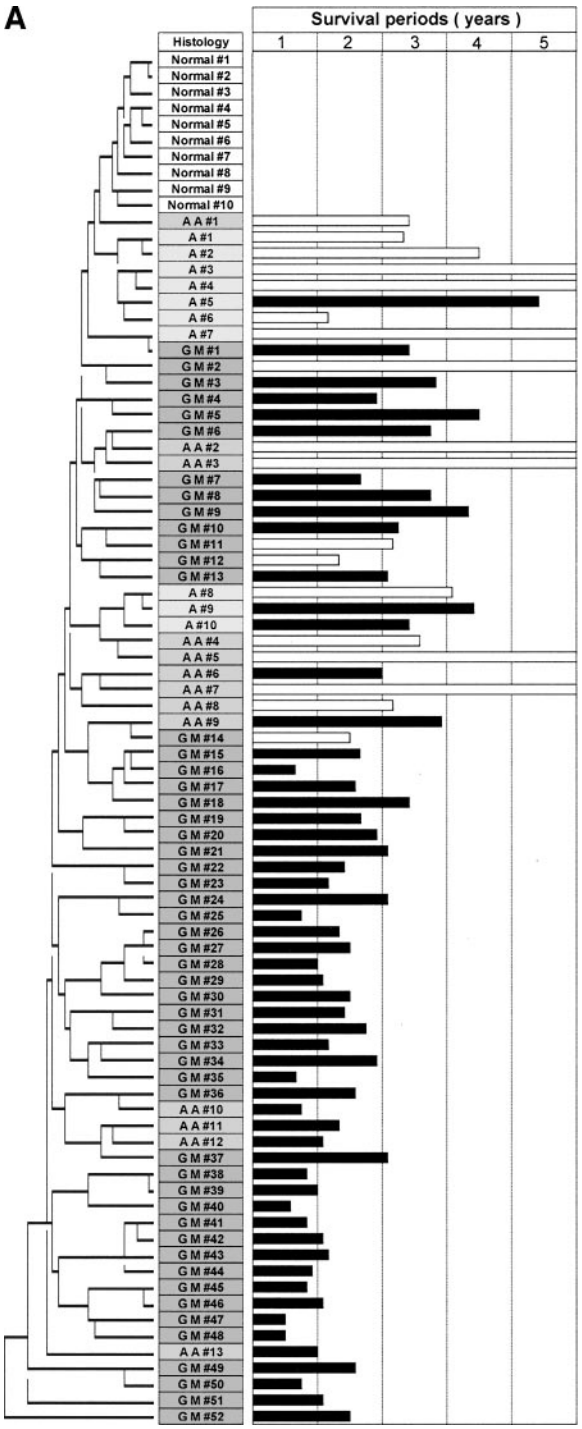

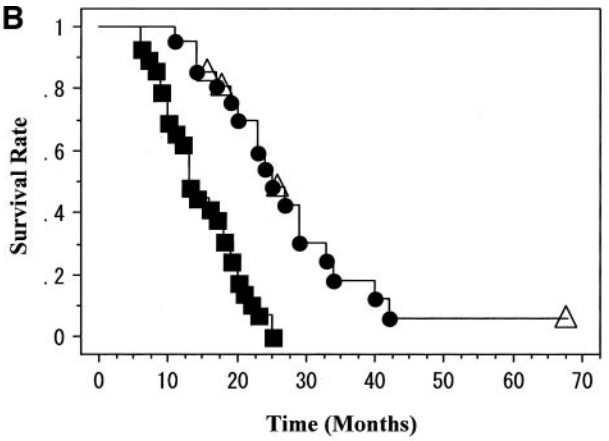

Fig. 3. *A*, hierarchical clustering based on proteome profiling data in the 75 glioma samples and 10 normal brain tissues. Each *row* represents a tissue sample, coding for the histological type of samples. *Normal*, normal brain tissue; *A*, astrocytoma; *AA*, anaplastic astrocytoma; *GM*, glioblastoma multiforme. The survival period of each patient is presented in the *right-hand column*: □ represents a surviving case; ■ represents a patient who had died. The median follow-up period for the surviving patients was 3.5 years. *B*, the 52 patients with glioblastoma multiforme (GM) were divided into two groups according to the branching patterns of the hierarchical clustering and the squared Euclidean distance coefficients with reference to the normal brain tissues. Kaplan–Meier survival curve analysis of 21 patients with GM that clustered near the normal brain tissues (●; *GM#1–GM#21* in *A*; coefficients <45.0) and the other 31 patients with GM that clustered relatively distant from the normal brain tissues (■; *GM#22–GM#52* in *A*; coefficients ≥ 45.0) is shown. The difference in the overall survival periods between the two groups was statistically significant ($P < 0.001$, log-rank test).

within 4 years after surgery. Samples from most patients with GM who had relatively long survival periods (>2 years) were also well categorized to an area near the normal brain tissue in the clustering map (Fig. 3*A*).

The 52 patients with GM were divided into two groups based on the branching patterns of the dendrogram and the squared Euclidean distance coefficient with reference to the normal brain tissues. We compared the overall survival periods between the two groups: the group with GM that was located near the normal brain tissues on the clustering map (21 patients) and the group with GM that was located relatively away from the normal brain tissues on the clustering map (31 patients; Fig. 3*B*). There were no significant differences between the two groups regarding potential prognostic factors such as age, performance status, extent of surgical resection, and dose administered in radiation therapy. The patients with GM located near the normal brain tissues on the clustering map lived significantly longer than the patients whose tumors were located distant from the normal brain tissues on the clustering map ($P < 0.001$, log-rank test). In accordance with the survival data, six cases in the latter group manifested leptomeningeal dissemination, whereas none of the former group showed such dissemination patterns ($P = 0.0321$, χ^2 test). This significant difference indicates that the tumors located distant from the normal brain tissues are more invasive in nature than the tumors located near the normal brain tissues in the proteome-based clustering.

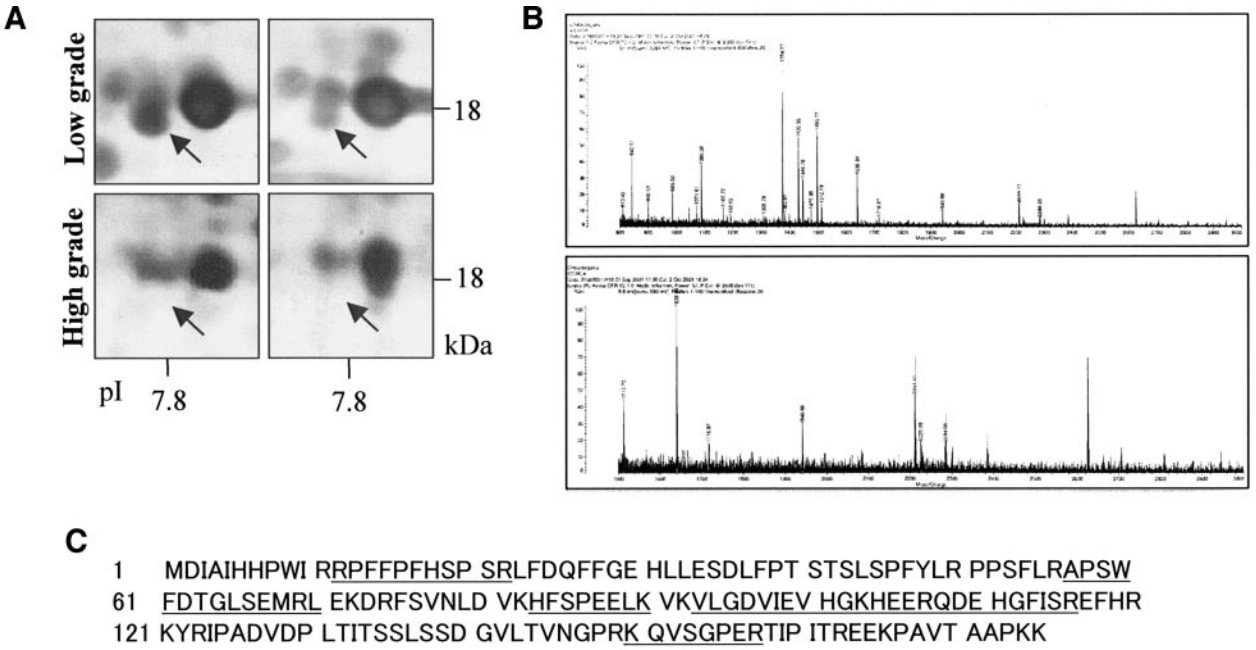

Fig. 4. Matrix-assisted laser desorption/ionization-time of flight mass spectrometric analysis of α-crystallin, which was expressed more frequently in the low-grade astrocytomas ($P = 0.0001$, discriminant analysis). *A*, representative two-dimensional gels. *B*, result of matrix-assisted laser desorption/ionization-time of flight mass spectrometric analysis. *C*, amino acid sequences analyzed by peptide mass fingerprinting analysis and *underlined* on the full-length sequence of the protein.

Identification of Proteins Associated with Malignant Progression in Gliomas. To identify the proteins that significantly correlated with histological grading, we performed discriminant analysis based on expression of the 257 protein spots. The selected protein spots were excised and analyzed by matrix-assisted laser desorption/ionization time-of-flight mass spectrometry (Fig. 4). Some protein spots could be identified by positive gel matching of protein expression patterns from several existing 2DE gel databases. Twenty-five known proteins and 12 unknown proteins were extracted from the analysis (Table 1). These 25 known proteins were functionally categorized, based on their known or inferred biological functions, into signal transduction-related proteins, molecular chaperones, transcription and translation regulators, cell cycle-mediating proteins, extracellular matrix-related proteins, and cell adhesion molecules.

Validation of Identified Proteins by Immunohistochemistry. The results of the proteome-based analysis for a subset of proteins related to tumor aggressiveness was confirmed by immunohistochemistry. Among the 37 specific proteins identified, antibodies to 5 were readily available for immunohistochemical analysis on paraffin-embedded sections. We observed high levels of cAMP-responsive element binding protein-1 in the nuclei of grade IV tumors, whereas other grade II tumors hardly stained with the antibody (Fig. 5). GRP78, Rho A, and Rac1 were also more abundantly expressed in the cytoplasm and processes of the tumor cells in the grade IV tumor cells compared with the lower grade tumors. In contrast, we observed higher levels of enolase in the lower grade tumors than the grade IV tumors, as indicated by the proteome analysis.

DISCUSSION

We examined the proteomes of human gliomas to establish a novel molecular classification that can distinguish aggressive tumors that are resistant to various treatments from the less-aggressive tumors among gliomas of the same histological grade. The results of hierarchical clustering analysis showed that tumor classification based on proteome profiling patterns could generate an accurate patient stratification that is more clinically relevant than the conventional histological classification. We consider proteome-based classification an efficient class-discovery tool for intracerebral gliomas, including survival prediction.

Because the functional molecules in the cell are proteins, proteome analysis based on 2DE would have several advantages over cDNA/oligonucleotide microarray systems for clinical use. First, the system measures primarily high-abundance proteins, which are ideal tumor biomarkers because they can be easily measured and targeted. mRNA levels are not directly associated with the amounts of functional proteins (10). Second, by use of proteomics, we can analyze the post-translational modifications that are essential for protein formation and function. For many proteins, post-translational modifications are important for their functions, and they can be analyzed only by the methods used in proteomics (11, 12). In contrast, 2DE analysis usually cannot detect hydrophobic membrane proteins, proteins larger than 100 kDa, or proteins with pI values outside the range 3–10. These limitations of standard 2DE could account for the failure of proteome analysis to identify proteins known to be overexpressed in glioma tissues, such as epidermal growth factor receptor, insulin-like growth factor binding protein 2, or vascular endothelial growth factor (6, 13).

Many small G-proteins have been reported to be involved in the malignant transformation of gliomas (14–16). The G-proteins bind to GTP and then activate a cascade of serine-threonine kinase, such as Raf and other so-called ras effectors, which transduce signals by cAMP-responsive element binding protein-1, a transcription regulator, resulting in alteration of the gene expressions (17). In the present study, eight small G-proteins were identified as related to malignant transformation. Among them, RalA, Rab3B, and nucleolar GTP-binding protein, recently recognized as a novel G-protein family, have not been reported as associated with the oncogenesis of gliomas. The up-regulated Rho family (RhoA and Rac1) may induce actin filament-mediated tumor cell migration as well as prevent apoptosis, in part through the ezrin/radixin/moesin group of proteins (14, 18). Recently,

Table 1 *Proteins identified as associated with histological grading of gliomas*

Accession no.	Entry name	Description	Function	pI	Mass (kDa)	*P*	Positive rate (*n*)	
							High grade	Low grade
High-grade glioma-associated proteins								
		Unknown	Unknown	7.45	88.6	0.0354	21/65	0/10
P15311	EZRI_HUMAN	Ezrin (p81; cytovillin)	Cytoskeleton/signal transduction	6.04	86.1	0.0064	38/65	1/10
P05129	KPCG_HUMAN	Protein kinase C γ	Signal transduction	8.1	79.5	0.0122	38/65	2/10
P11021	GR78_HUMAN	78-kDa glucose-regulated protein (GRP78)	Molecular chaperone	4.99	75.7	0.0061	48/65	2/10
Q9BZE4	NOG1_HUMAN	Nucleolar GTP-binding protein	GTP-binding protein	5.04	74.1	0.0283	25/65	0/10
		Unknown	Unknown	8.03	69.5	0.0001	49/65	1/10
		Unknown	Unknown	7.87	68.6	0.0018	32/65	0/10
P05121	PAI1_HUMAN	Plasminogen activator inhibitor-1	Protease	6.96	48.3	0.0337	44/65	3/10
P04765	IF41_HUMAN	Eukaryotic initiation factor 4A (p37)	Translation regulation	4.95	46.1	0.0001	40/65	0/10
		Unknown	Unknown	4.71	45.9	0.0162	45/65	3/10
		Unknown	Unknown	4.56	45.2	0.0001	56/65	3/10
Q02750	MPK1_HUMAN	MAPK[a]/ERK kinase 1	Signal transduction	6.76	43.3	0.0233	34/65	1/10
		Unknown	Unknown	4.42	41.3	0.0071	54/65	4/10
P07355	ANX2_HUMAN	Annexin II (lipocortin II)	Phospholipid-binding protein	7.12	38.5	0.006	50/65	3/10
P16220	CREB_HUMAN	cAMP-response element binding protein-1	Transcription regulation	6.2	36.6	0.0032	52/65	3/10
P09525	ANX4_HUMAN	Annexin IV (lipocortin IV)	Phospholipid-binding protein	5.6	35.8	0.0328	26/65	0/10
P07339	CATD_HUMAN	Cathepsin D	Protease/apoptosis induction	5.63	34.1	0.0443	38/65	2/10
P35232	PHB_HUMAN	Prohibitin	Molecular chaperone	5.74	29.8	0.0017	48/65	2/10
P18669	PGM1_HUMAN	Phosphoglycerate mutase 1	Metabolic enzyme	6.67	28.6	0.0001	60/65	4/10
P09488	GTM1_HUMAN	Glutathione *S*-transferase M	Metabolic enzyme	7.35	25.6	0.0025	57/65	4/10
P20336	RB3A_HUMAN	RAB3A, member *RAS* oncogene family	GTP-binding protein	8.31	24.9	0.0474	46/65	3/10
P11233	PALA_HUMAN	Ras-related protein Ral-A	GTP-binding protein	7.05	23.6	0.0352	49/65	4/10
P04792	HS27_HUMAN	Heat shock 27-kDa protein (HSP27)	Molecular chaperone	5.61	22.8	0.0019	37/65	0/10
P06749	RHOA_HUMAN	Transforming protein Rho A	GTP-binding protein	6.35	21.8	0.0024	58/65	4/10
P15154	RAC1_HUMAN	Rac1	GTP-binding protein	8.1	21.5	0.0001	55/65	2/10
		Unknown	Unknown	8.06	20.3	0.0002	51/65	2/10
		Unknown	Unknown	8.16	19.4	0.0453	27/65	0/10
Low-grade glioma-associated proteins								
		Unknown	Unknown	6.5	82.1	0.0009	28/65	10/10
		Unknown	Unknown	8.06	67.6	0.0246	26/65	8/10
P00367	DHE3_HUMAN	Glutamate dehydrogenase 1	Metabolic enzyme	7.26	61.3	0.0063	27/65	9/10
P30101	PDA3_HUMAN	Protein disulfide isomerase A3	Molecular chaperone	4.76	56.8	0.0015	21/65	9/10
P06733	ENOA_HUMAN	Phosphopyruvate hydratase	Metabolic enzyme	7.01	47	0.0001	16/65	6/10
		Unknown	Unknown	8.04	39.8	<0.0001	15/65	10/10
		Unknown	Unknown	7.06	39.2	<0.0001	19/65	10/10
P09211	GTP_HUMAN	Glutathione *S*-transferase P	Metabolic enzyme	5.43	23.3	0.0021	22/65	9/10
P02511	CRAB_HUMAN	α Crystallin B chain	Cytoskeleton/molecular chaperone	6.84	20.2	0.0001	23/65	10/10
P38936	CDN1_HUMAN	Cyclin-dependent kinase inhibitor 1 (p21)	Cell cycle regulation	7.92	19.7	0.0369	20/65	8/10

[a] MAPK, mitogen-activated protein kinase; ERK, extracellular signal-regulated kinase.

Senger *et al.* (15) emphasized that Rac1 regulates a major survival pathway in most human gliomas and that suppression of Rac1 activity induces death in glioma cells. These results suggest that despite the lack of oncogenic ras mutations in astrocytomas, aberrant G-protein signaling plays a crucial role in malignant transformation of gliomas and would be a rational target for antiglioma therapy.

Chaperone proteins reduce stress-induced denaturation and aggregation of intracellular proteins and are reported to exert protective

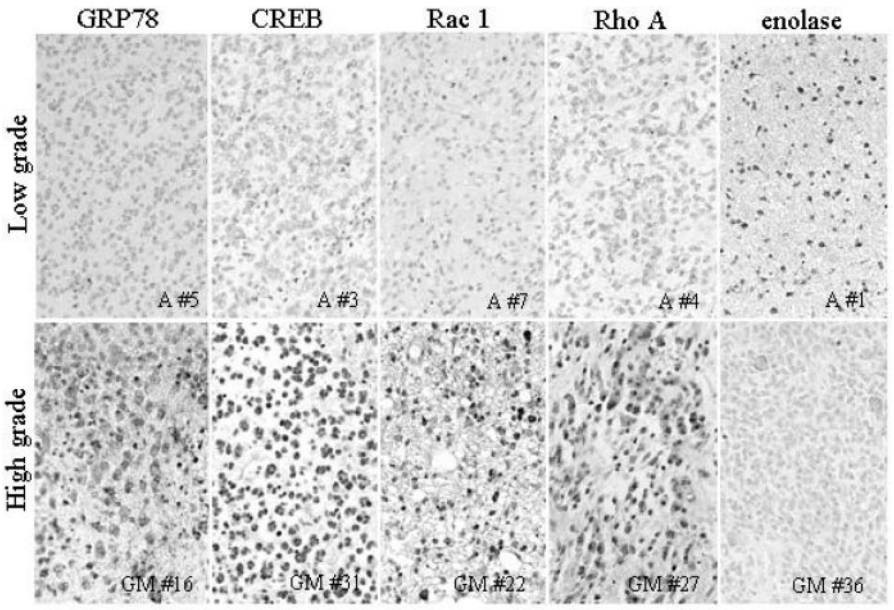

Fig. 5. Immunohistochemical analysis of the expression of GRP78, cAMP-responsive element binding protein-1 (*CREB*), Rac1, RhoA, and enolase in the paraffin-embedded sections of 10 cases: 5 cases with high-grade astrocytomas (*GM#16*, *GM#22*, *GM#27*, *GM#31*, and *GM#36*) and 5 cases with low-grade astrocytomas (*A#1*, *A#3*, *A#4*, *A#5*, and *A#7*). cAMP response element-binding protein-1 was detected in the nuclei of high-grade tumors but was weakly positive in low-grade tumors. GRP78, Rac1, and RhoA were abundantly expressed in the cytoplasm of high-grade tumors but were scarcely detected in low-grade tumors. In contrast, enolase was highly expressed in low-grade tumors compared with high-grade tumors.

actions by interfering with the stress-induced apoptotic pathway in healthy neuronal cells (19). The results obtained in our study show that chaperone proteins work diversely in glioma cells; GRP78, prohibitin, and heat shock protein 27 were associated with high-grade tumors, whereas protein disulfide isomerase and α-crystallin were associated with low-grade tumors. Various proteases and their inhibitors were also found to be important in glioma invasion and angiogenesis. The plasminogen activator system, including plasminogen activator inhibitor type 1, was previously demonstrated to be associated with higher grades of glioma (20). This system interacts with annexin II, which is known to be an independent prognostic factor for poor outcome in gliomas (21, 22). We ascertained in the present study that the expression of plasminogen activator inhibitor type 1, annexin II, annexin IV, and cathepsin D proteins was increased in high-grade gliomas.

We have shown a novel system of classification based on protein expression by analyzing 75 glioma specimens with 2DE-based proteome analysis. Our results also demonstrate that the biological characteristics of intracerebral glioma are defined by numerous proteins, which implies that the aggressiveness of gliomas can not be predicted by single or small numbers of protein markers but rather by combinations of many proteins. Many of the identified proteins work in signal transduction and as molecular chaperones. These proteins could be predictive markers for the aggressiveness of gliomas and could be direct and rational targets for antiglioma therapy.

ACKNOWLEDGMENTS

We thank Noriyuki Ozima and Minoru Yamaguchi (Shimadzu Co., Ltd.) for technical assistance in the matrix-assisted laser desorption/ionization time-of-flight mass spectrometry analysis using AXIMA-CFR.

REFERENCES

1. Cavenee WK, Weller M, Furnari FB, et al. Diffuse infiltrating astrocytomas. In: Cavenee WK, Kleihues P, editors. Pathology & genetics of tumors of nervous system. Lyon: IARC Press, 2000. p. 9–15.
2. Alizadeh AA, Eisen MB, Davis RE, et al. Distinct types of diffuse large B-cell lymphoma identified by gene expression profiling. Nature (Lond) 2000;403:503–11.
3. Bittner M, Meltzer P, Chen Y, Jiang Y, Sondak V. Molecular classification of cutaneous malignant melanoma by gene expression profiling. Nature (Lond) 2000; 406:536–40.
4. Pomeroy SL, Tamayo P, Gaasenbeek M, Sturla LM, Golub TR. Prediction of central nervous system embryonal tumour outcome based on gene expression. Nature (Lond) 2002;415:436–42.
5. Rickman DS, Bobek MP, Misek DE, et al. Distinctive molecular profiles of high-grade and low-grade gliomas based on oligonucleotide microarray analysis. Cancer Res 2001;61:6885–91.
6. Sallinen SL, Sallinen PK, Haapasalo HK, et al. Identification of differentially expressed genes in human gliomas by DNA microarray and tissue chip techniques. Cancer Res 2000;60:6617–22.
7. Celis JE, Gromov P, Ostergaard M, et al. Human 2-D PAGE databases for proteome analysis in health and disease: http://biobase.dk/cgi-bin/celis. FEBS Lett 1996;398: 129–34.
8. Sanchez JC, Rouge V, Pisteur M, et al. Improved and simplified in-gel sample application using reswelling of dry immobilized pH gradients. Electrophoresis 1997; 18:324–7.
9. Wolfsberg TG, Wetterstrand KA, Guyer MS, Collins FS, Baxevanis AD. A user's guide to the human genome. Nat Genet 2002;32(Suppl):1–79.
10. Futcher B, Latter GI, Monardo P, McLaughlin CS, Garrels JIA. sampling of the yeast proteome. Mol Cell Biol 1999;19:7357–68.
11. Sali A. Functional links between proteins. Nature (Lond) 1999;402:23–6.
12. Oliver S. Guilt-by-association goes global. Nature (Lond) 2000;403:601–3.
13. Berkman RA, Merrill MJ, Reinhold WC, et al. Expression of the vascular permeability factor/vascular endothelial growth factor gene in central nervous system neoplasms. J Clin Investig 1993;91:153–9.
14. Woods SA, Marmor E, Feldkamp M, et al. Aberrant G protein signaling in nervous system tumors. J Neurosurg 2002;97:627–42.
15. Senger DL, Tudan C, Guiot MC, et al. Suppression of Rac activity induces apoptosis of human glioma cells but not normal human astrocytes Cancer Res 2002;62: 2131–40.
16. Ding H, Roncari L, Shannon P, et al. Astrocyte-specific expression of activated p21-ras results in malignant astrocytoma formation in a transgenic mouse model of human gliomas. Cancer Res 2001;61:3826–36.
17. Bleckmann SC, Blendy JA, Rudolph D, Monaghan AP, Schmid W, Schutz G. Activating transcription factor 1 and CREB are important for cell survival during early mouse development. Mol Cell Biol 2002;22:1919–25.
18. Ridley AJ. RHO. Theme and variation. Curr Biol 1996;6:1256–64.
19. Houry WA. Chaperone-assisted protein folding in the cell cytoplasm. Curr Protein Pept Sci 2001;2:227–44.
20. Muracciole X, Romain S, Dufour H, et al. PAI-1 and EGFR expression in adult glioma tumors: toward a molecular prognostic classification. Int J Radiat Oncol Biol Phys 2002;52:592–8.
21. Siao CJ, Tsirka SE. Tissue plasminogen activator mediates microglial activation via its finger domain through annexin II. J Neurosci 2002;22:3352–8.
22. Reeves SA, Chavez-Kappel C, Davis R, Rosenblum M, Israel MA. Developmental regulation of annexin II (Lipocortin 2) in human brain and expression in high grade glioma. Cancer Res 1992;52:6871–6.

Molecular Classification and Survival Prediction in Human Gliomas Based on Proteome Analysis

Yasuo Iwadate, Tsukasa Sakaida, Takaki Hiwasa, et al.

Cancer Res 2004;64:2496-2501.